Acta Cryst E CRYSTALLOGRAPHIC COMMUNICATIONS

ISSN 2056-9890

Synthesis, crystal structure and Hirshfeld surface analysis of a polymeric bismuthate(III) halide complex, $(C_6H_6N_3)_2[BiCl_5]\cdot 2H_2O$

Chaima Boukoum,[a]* Zouhaier Aloui,[a] Valeria Ferretti[b] and Sonia Abid[a]

[a]Laboratoire de Chimie des Matériaux, Faculté des Sciences de Bizerte, 7021 Zarzouna Bizerte, Tunisia, and [b]Department of Chemical and Pharmaceutical Sciences, Centre for Structural, Diffractometry, University of Ferrara, Via L. Borsari 46, I-44121 Ferrara, Italy. *Correspondence e-mail: ch.boukoum@gmail.com

Received 8 October 2017
Accepted 17 October 2017

Edited by W. T. A. Harrison, University of Aberdeen, Scotland

Keywords: crystal structure; halogenobismuthates; benzotriazole; Hirshfeld surface analysis.

CCDC reference: 1580458

Supporting information: this article has supporting information at journals.iucr.org/e

The synthesis and the crystal structure of a new halide-bridged polymer, namely *catena*-poly[bis(1,2,3-benzotriazolium) [[tetrachloridobismuth(III)]-μ-chlorido] dihydrate], $\{(C_6H_6N_3)_2[BiCl_5]\cdot 2H_2O\}_n$ are reported. The structure comprises polyanionic zigzag chains of formula $[(BiCl_5)^{2-}]_n$ running along the *c*-axis direction. The 1,2,3-benzotriazolium cations are linked between these polymer chains, *via* the water molecules, giving rise to left- and right-handed helical chains. Hirshfeld surface analysis and fingerprint plots were used to decode the intermolecular interactions in the crystal network and determine the contribution of the component units for the construction of the three-dimensional architecture.

1. Chemical context

Bismuth–halide complexes are of contemporary interest because of their structural diversity and numerous promising physical properties such as dielectric, ferroelectric, ferroelastic, non-linear optical and thermochromism (Bator *et al.*, 1997; Bednarska-Bolek *et al.*, 2000; Sobczyk *et al.*, 1997; Bator *et al.*, 1998). Generally, in these compounds, the BiX_6 octahedra may join to form discrete (*i.e.* mononuclear) or extended (*i.e.* polynuclear) inorganic networks of corner-, edge-, or face-sharing octahedra, leading to an extensive family of bismuth halogenoanions (Jakubas, 1986; Jakubas *et al.*, 1988, 1995). A variety of organic cations, ring shaped or linear, have a strong impact on the arrangements of BiX_6 octahedra and the formation of hydrogen bonds (Dammak *et al.*, 2015; Elfaleh & Kamoun, 2014). This class of compounds has also attracted much attention in the field of crystal engineering over the last decade on account of their capability for the creation of extended architectures *via* intermolecular non-covalent binding interactions. (*i.e.* hydrogen bonding, ionic and π–π stacking interactions; Belter & Fronczek, 2013; Thirunavukkarasu *et al.*, 2013; Aloui *et al.*, 2015).

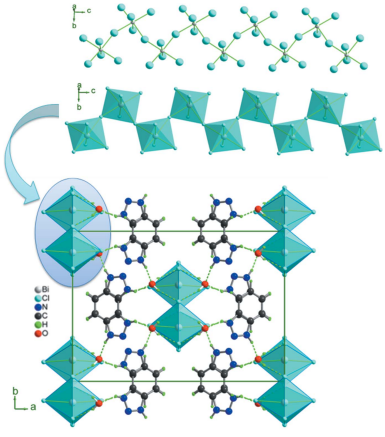

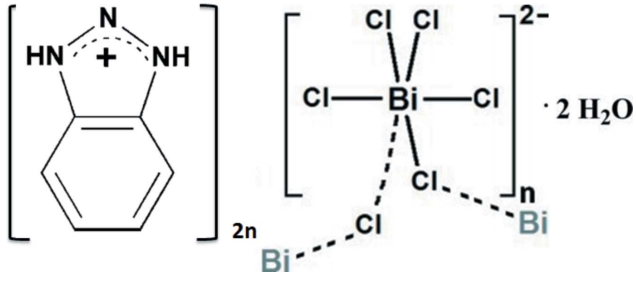

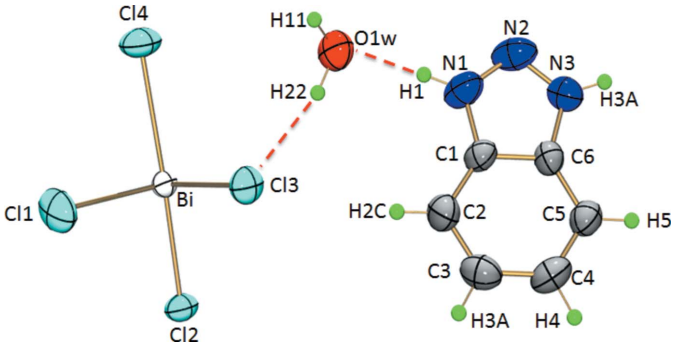

Figure 1
The asymmetric unit of (I) showing 50% displacement ellipsoids.

As part of our studies in this area, we chose benzotriazole, which is an aromatic heterocyclic base with three protonatable nitrogen atoms, as the organic cation.

2. Structural commentary

The single-crystal X-ray diffraction analysis shows that the title compound $[C_6H_6N_3]_2[BiCl_5]\cdot 2H_2O$, (I), crystallizes in the non-centrosymmetric space group $Cmc2_1$ and the asymmetric unit comprises one Bi^{3+} cation, four chlorine atoms, one water molecule and one benzotriazolium cation (Fig. 1). The bismuth atom is six-coordinated by four distinct chlorine atoms (Cl1, Cl2, Cl3, Cl4). The Bi—Cl bond lengths (Table 1) vary from 2.545 (3) to 2.674 (4) Å (ΔBi—Cl = 0.129 Å) and 2.757 (4) to 2.856 (4) Å (ΔBi—Cl = 0.099 Å) for non-bridging and bridging Cl atoms, respectively, which are comparable with values found in $\{(C_2H_7N_4O)_2[BiCl_5]\}_n$ (Ferjani *et al.*, 2012) and $[NH_3(CH_2)_6NH_3]BiCl_5$ (Ouasri *et al.*, 2013). The Cl—Bi—Cl bond angles in (I) range from 85.93 (17) to 91.88 (13)° (ΔCl—Bi—Cl =5.95°) and are less distorted than those observed in $[NH_3(CH_2)_6NH_3]BiCl_5$ and $[H_2mdap][BiCl_5]$ (Ouasri *et al.*, 2013; Wang *et al.*, 2017).

Table 1
Selected bond lengths (Å).

Bi1—Cl1	2.669 (3)	Bi1—Cl4^{i}	2.757 (4)
Bi1—Cl2	2.545 (3)	Bi1—Cl4	2.856 (4)
Bi1—Cl3	2.674 (4)		

Symmetry code: (i) $-x+1, -y+1, z-\frac{1}{2}$.

In the extended structure of (I), adjacent $BiCl_6$ octahedra are connected through Cl4 and Cl4^{iii} so as to form $[(BiCl_5)^{2-}]_n$ polyanionic zigzag chains propagating along the c-axis direction, with the shortest intra-chain Bi···Bi distance of 5.508 (1) Å and a Cl4—Bi—Cl4^{ii} angle of 89.61 (3)° (Fig. 2) The overall negative charges of the resulting polymers are counter-balanced by the protonated 1,2,3-benzotriazolium cations (Fig. 2*b*). As usual, this aromatic amine is protonated at the N3 atom and the C—C, N—N and C—N bond lengths vary from 1.358 (18) to 1.402 (15), 1.293 (15) to 1.308 (15) Å and 1.364 (16) to 1.370 (15) Å, respectively, which agree well with those observed in bis(1,2,3-benzotriazolium) sulfate dihydrate (Randolph *et al.*, 2013) and benzotriazolium picrate (Zeng *et al.*, 2011).

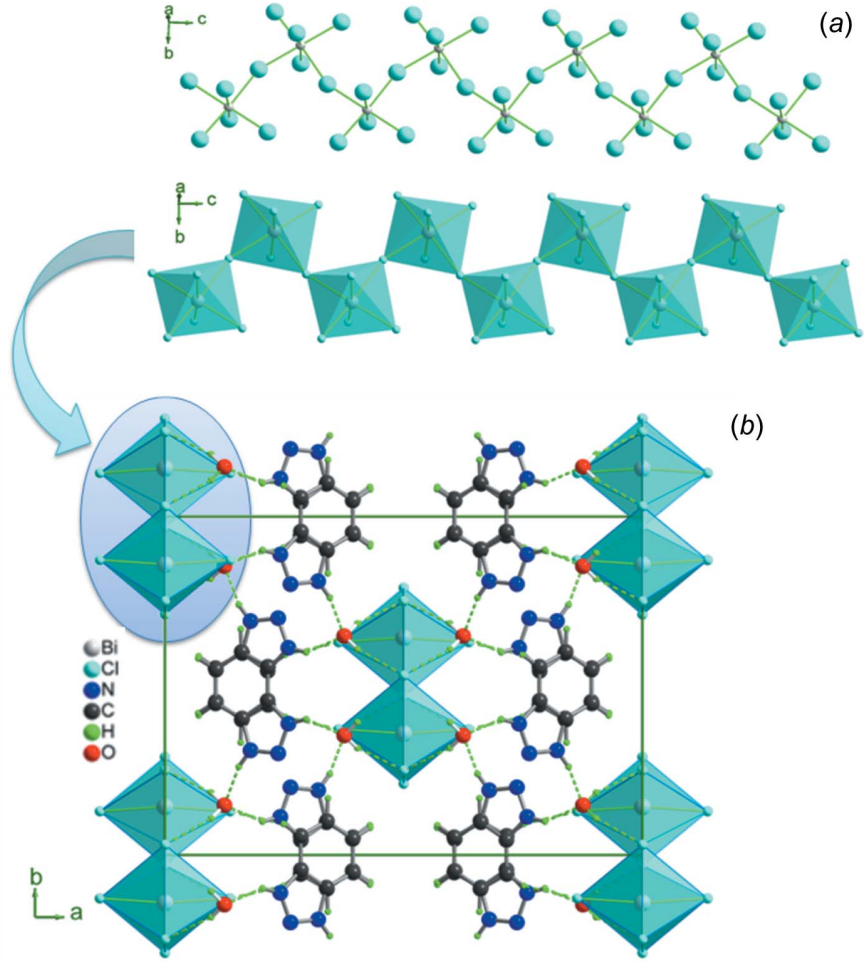

Figure 2
(*a*) View of the $[(BiCl_5)^{2-}]_n$ polyanionic zigzag chains in (I) along the *c*-axis direction. (*b*) Projection along the *c* axis of the structure of (I).

3. Supramolecular features

The heterocyclic cations alternately bridge the water molecules (O1*W*) *via* N—H···O hydrogen bonds, forming $(benzo\text{-}OW)_n$ helical chains in a right- and left–handed sequence extending along the *c*-axis direction (Table 2, Fig. 2). The phenyl rings of adjacent chains are alternately stacked in a parallel-displaced face-to-face arrangement (Fig. 3), with centroid–centroid distances of 3.8675 (1) Å and an inter-planar spacing of 1.13 Å. The anionic

Table 2
Hydrogen-bond geometry (Å, °).

D—H···A	D—H	H···A	D···A	D—H···A
N1—H1···O1W	0.86	2.08	2.891 (17)	157
N3—H3A···O1W^{ii}	0.86	2.00 (2)	2.767 (18)	148
O1W—H11···Cl4^{iii}	0.89 (11)	2.47 (11)	3.306 (13)	157 (9)
O1W—H22···Cl3	0.90 (12)	2.38 (12)	3.268 (14)	169 (11)
C5—H5···Cl1^{iv}	0.93	2.73	3.603 (14)	157

Symmetry codes: (ii) $-x+\frac{3}{2}, -y+\frac{1}{2}, z+\frac{1}{2}$; (iii) $-x+1, -y+1, z+\frac{1}{2}$; (iv) $x+\frac{1}{2}, y-\frac{1}{2}, z+1$.

and cationic chains are further assembled into a three-dimensional supramolecular framework through N—H···O, O—H···Cl and C—H···Cl hydrogen bonds (Table 2, Fig. 3).

4. Hirshfeld surface analysis

The Hirshfeld surface (Wolff *et al.*, 2012) mapped with a d_{norm} function for the asymmetric unit for the title compounds clearly shows the red spots derived from H···O and H···Cl/Cl···H contacts (Fig. 4). The two-dimensional fingerprint plot shows that the H···Cl/Cl···H contacts associated with O—H···Cl hydrogen bonding appear to be the major contributor in the crystal packing (55.8%): these contacts are represented as regions in the top left ($d_e > d_i$, Cl···H) and bottom right ($d_e < d_i$, H···Cl) of the related plots in Fig. 5. Interactions of

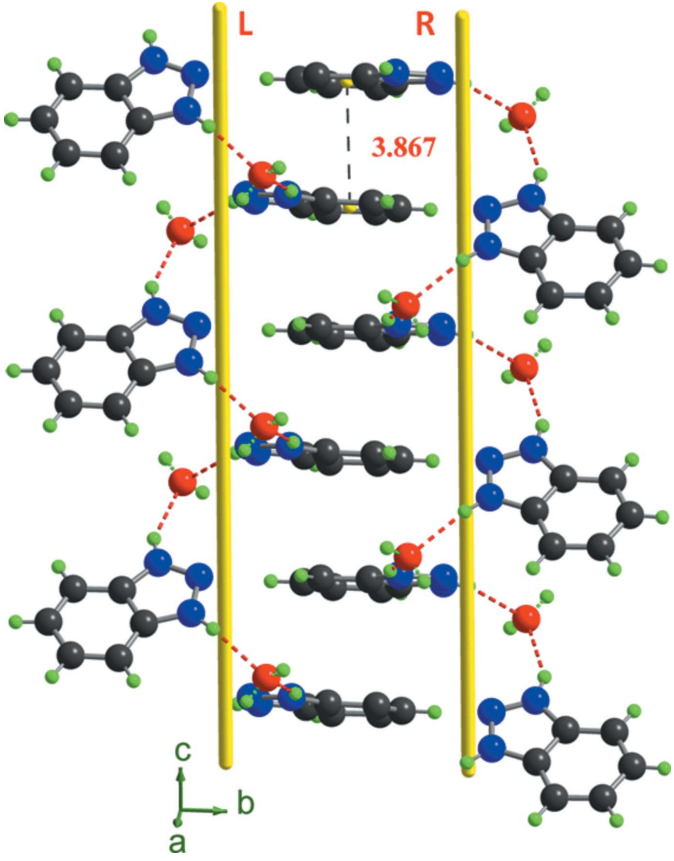

Figure 3
View of the infinite helical hydrogen-bonded chain in (I).

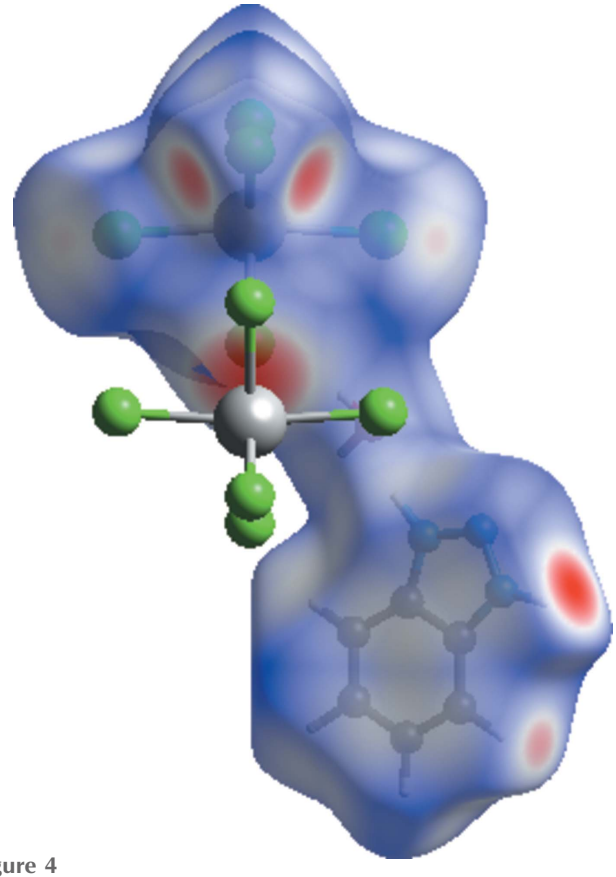

Figure 4
Hirshfeld surface mapped over d_{norm} of (I).

the type H···H appear in the middle of the scattered points in the fingerprint maps; they comprise 10.9% of the entire surface. The decomposition of the fingerprint plot shows that N···H/H···N, C···H/H···C, O···H/H···O and N···Cl/Cl···N contacts have percentage contributions of 7.8%, 6.5%, 4.5% and 4.3% respectively, of the total Hirshfeld surface. The C···C contacts associated with π–π interactions amount to 3.4% of the surface: their presence is indicated by the appearance of red and blue triangles on the shape-indexed surfaces in Fig. 6. The Cl···Bi/Bi···Cl (3%) interactions are represented as points in the top area. The Cl···Cl, C···Cl/Cl···C, C···N, and N···N interactions are in the middle of the fingerprint plots, and comprise a very small contribution of 1.3%, 1.2%, 0.9% and 0.4%, respectively.

The intermolecular interactions were further evaluated by using the enrichment ratio (ER; Jelsch *et al.*, 2014). The largest contribution to the Hirshfeld surface is from H···Cl/Cl···H contacts associated with O—H···Cl hydrogen bonds and their ER value is 1.73. The H···H contacts are the second largest contributor, but they display an enrichment ratio significantly below unity (ER_{HH} = 0.47). The formation of extensive π–π interactions is reflected in the relatively high ER_{CC} of 3.94.

5. Synthesis and crystallization

The title compound was prepared by dropwise addition of an ethanolic solution of 1*H*-benzotriazole (0.061 g, 0.5 mmol) to

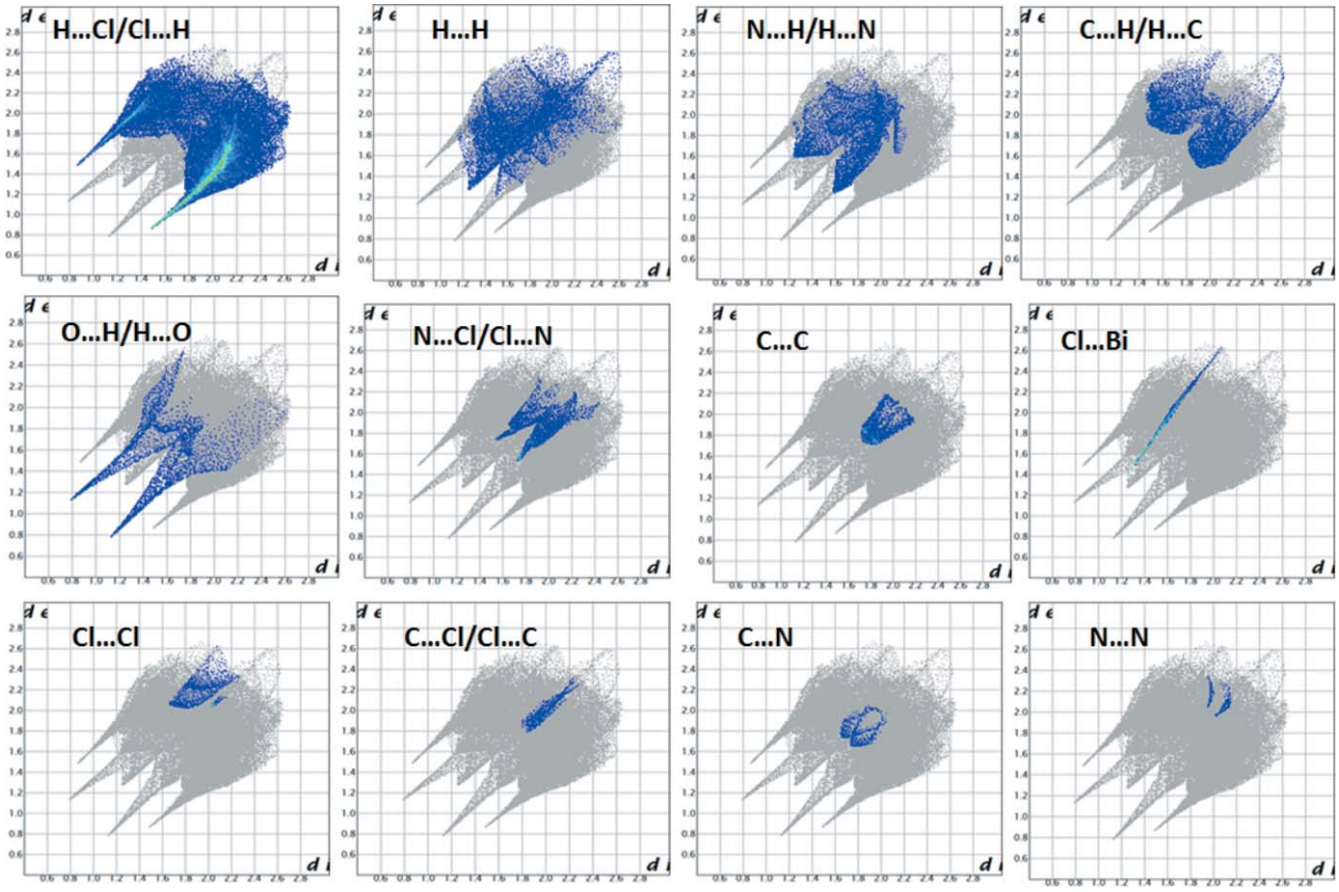

Figure 5
Two-dimensional fingerprint plots for (I) showing contributions from different contacts.

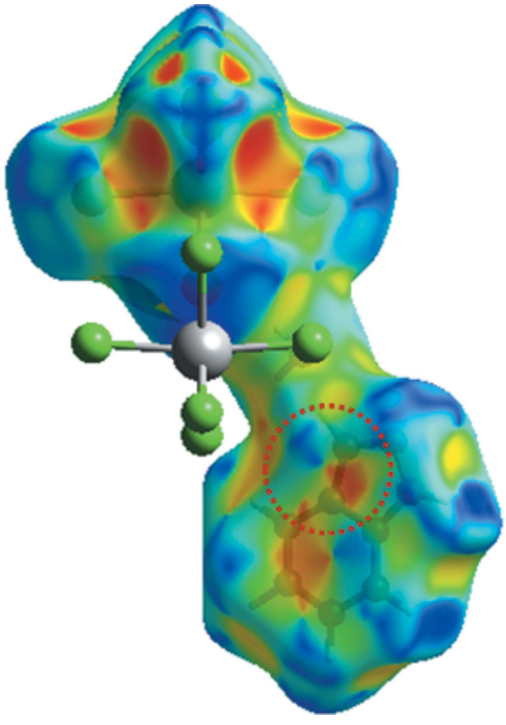

Figure 6
Hirshfeld surface mapped over the shape index for (I) highlighting the regions involved in π-π stacking interactions.

1 mmol of a bismuth nitrate solution [$Bi(NO_3)_3{\cdot}5H_2O$], dissolved in 0.05 mL of a concentrated HCl aqueous solution. The resulting aqueous solution was stirred for 30 min. and kept at room temperature for crystallization. After two week of slow evaporation, colourless single crystals of (I) (yield = 75%) were formed in the solution. Analysis observed (calculated) for $[C_6H_6N_3]_2[BiCl_5]{\cdot}2H_2O$ (%): C 21.6 (21.0), H 2.66 (2.41), N 34.6 (33.8).

6. Refinement

Crystal data, data collection and structure refinement details are summarized in Table 3. The N-bound and C-bound hydrogen atoms were positioned geometrically and treated as riding: N—H = 0.86 Å and C—H = 0.93 Å with U_{iso}(H) = 1.2U_{eq}(N,C). The O—H and H···H separations in the water molecule were restrained using a DFIX model to be 0.90 and 1.46 Å, respectively, and refined with U_{iso}(H) = 1.5U_{eq}(O).

Acknowledgements

This work was supported by the Tunisian Ministry of High Education Scientific Research.

References

Aloui, Z., Ferretti, V., Abid, S., Lefebvre, F., Rzaigui, M. & Nasr, C. B. (2015). *J. Mol. Struct.* **1097**, 166–170.

Bator, G., Baran, J., Jakubas, R. & Sobczyk, L. (1998). *J. Mol. Struct.* **450**, 89–100.

Bator, G., Provoost, R., Silverans, R. E. & Zeegers-Huyskens, Th. (1997). *J. Mol. Struct.* **435**, 1–10.

Bednarska-Bolek, B., Zaleski, J., Bator, G. & Jakubas, R. (2000). *J. Phys. Chem. Solids*, **61**, 1249–1261.

Belter, R. K. & Fronczek, F. R. (2013). *Acta Cryst.* E**69**, o606–o607.

Blessing, R. H. (1995). *Acta Cryst.* A**51**, 33–38.

Burnett, M. N. & Johnson, C. K. (1996). *ORTEPIII*. Report ORNL-6895. Oak Ridge National Laboratory, Tennessee, USA.Dammak, H., Feki, H., Boughzala, H. & Abid, Y. (2015). *Spectrochim. Acta A Mol. Biomol. Spectrosc.* **137**, 1235–1243.

Farrugia, L. J. (2012). *J. Appl. Cryst.* **45**, 849–854.

Elfaleh, N. & Kamoun, S. (2014). *J. Mol. Struct.* **1075**, 479–485.

Ferjani, H., Boughzala, H. & Driss, A. (2012). *Acta Cryst.* E**68**, m615.

Flack, H. D. (1983). *Acta Cryst.* A**39**, 876–881.

Jakubas, R. (1986). *Solid State Commun.* **60**, 389–391.

Jakubas, R., Bator, G. & Mróz, J. (1995). *Acta Phys. Pol. A*, **87**, 663–669.

Jakubas, R., Krzewska, U., Bator, G. & Sobczyk, L. (1988). *Ferroelectrics*, **77**, 129–135.

Jelsch, C., Ejsmont, K. & Huder, L. (2014). *IUCrJ*, **1**, 119–128.

Nonius (1997). *KappaCCD Server Software for Windows*. Nonius BV, Delft, The Netherlands.

Otwinowski, Z. & Minor, W. (1997). *Methods in Enzymology*, Vol. 276, *Macromolecular Crystallography*, Part A, edited by C. W. Carter Jr & R. M. Sweet, pp. 307–326. New York: Academic Press.

Ouasri, A., Jeghnou, H., Rhandour, A. & Roussel, P. (2013). *J. Solid State Chem.* **200**, 22–29.

Sheldrick, G. M. (2008). *Acta Cryst.* A**64**, 112–122.

Sobczyk, L., Jakubas, R. & Zaleski, J. (1997). *Pol. J. Chem.* **71**, 265–300.

Thirunavukkarasu, A., Silambarasan, A., Chakkaravarthi, G., Mohankumar, R. & Umarani, P. R. (2013). *Acta Cryst.* E**69**, o1605.

Wang, Y., Shi, C. & Han, X. (2017). *Polyhedron*, **133**, 132–136.

Table 3
Experimental details.

Crystal data	
Chemical formula	$(C_6H_6N_3)_2[BiCl_5]\cdot 2H_2O$
M_r	662.54
Crystal system, space group	Orthorhombic, $Cmc2_1$
Temperature (K)	293
a, b, c (Å)	19.4627 (4), 13.8181 (4), 7.7343 (2)
V (Å^3)	2080.04 (9)
Z	4
Radiation type	Mo $K\alpha$
μ (mm^{-1})	9.14
Crystal size (mm)	0.55 × 0.34 × 0.23
Data collection	
Diffractometer	Nonius KappaCCD
Absorption correction	Multi-scan (*SORTAV*; Blessing, 1995)
T_{min}, T_{max}	0.011, 0.053
No. of measured, independent and observed [$I > 2\sigma(I)$] reflections	6050, 1670, 1643
R_{int}	0.067
$(\sin\theta/\lambda)_{max}$ (Å^{-1})	0.581
Refinement	
$R[F^2 > 2\sigma(F^2)]$, $wR(F^2)$, S	0.038, 0.096, 1.11
No. of reflections	1670
No. of parameters	131
No. of restraints	4
H-atom treatment	H atoms treated by a mixture of independent and constrained refinement
$\Delta\rho_{max}$, $\Delta\rho_{min}$ (e Å^{-3})	1.68, −0.76
Absolute structure	Flack (1983), 731 Friedel pairs
Absolute structure parameter	−0.036 (14)

Computer programs: Kappa CCD server software (Nonius, 1997), *DENZO-SMN* (Otwinowski & Minor, 1997), *SHELXS97*, *SHELXL97* and *SHELXTL* (Sheldrick, 2008), *ORTEPIII* (Burnett & Johnson, 1996), and *WinGX* (Farrugia, 2012).

Wolff, S. K., Grimwood, D. J., McKinnon, J. J., Turner, M. J., Jayatilaka, D. & Spackman, M. A. (2012). *CrystalExplorer*. University of Western Australia.

Zeng, B., Li, J. & Wang, G. (2011). *Acta Cryst.* E**67**, o1464.

supporting information

Acta Cryst. (2017). E**73**, 1759-1763 [https://doi.org/10.1107/S2056989017015134]

Synthesis, crystal structure and Hirshfeld surface analysis of a polymeric bismuthate(III) halide complex, $(C_6H_6N_3)_2[BiCl_5]\cdot 2H_2O$

Chaima Boukoum, Zouhaier Aloui, Valeria Ferretti and Sonia Abid

Computing details

Data collection: Kappa CCD server software (Nonius, 1997); cell refinement: *DENZO-SMN* (Otwinowski & Minor, 1997); data reduction: *DENZO-SMN* (Otwinowski & Minor, 1997); program(s) used to solve structure: *SHELXS97* (Sheldrick, 2008); program(s) used to refine structure: *SHELXL97* (Sheldrick, 2008); molecular graphics: *ORTEPIII* (Burnett & Johnson, 1996); software used to prepare material for publication: *SHELXTL* (Sheldrick, 2008) and *WinGX* (Farrugia, 2012).

***catena*-Poly[bis(1,2,3-benzotriazolium) [[tetrachloridobismuth(III)]-μ-chlorido] dihydrate]**

Crystal data

$(C_6H_6N_3)_2[BiCl_5]\cdot 2H_2O$
$M_r = 662.54$
Orthorhombic, $Cmc2_1$
Hall symbol: C 2c -2
$a = 19.4627$ (4) Å
$b = 13.8181$ (4) Å
$c = 7.7343$ (2) Å
$V = 2080.04$ (9) Å^3
$Z = 4$
$F(000) = 1256$
$D_x = 2.116$ Mg m^{-3}
Mo $K\alpha$ radiation, $\lambda = 0.71073$ Å
Cell parameters from 8027 reflections
$\theta = 4.4$–$7.3°$
$\mu = 9.14$ mm^{-1}
$T = 293$ K
Rod, colourless
0.55 × 0.34 × 0.23 mm

Data collection

Nonius KappaCCD diffractometer
Radiation source: fine-focus sealed tube
Graphite monochromator
f scans and w scans
Absorption correction: multi-scan (SORTAV; Blessing, 1995)
$T_{min} = 0.011$, $T_{max} = 0.053$
6050 measured reflections
1670 independent reflections
1643 reflections with $I > 2\sigma(I)$
$R_{int} = 0.067$
$\theta_{max} = 24.4°$, $\theta_{min} = 4.4°$
$h = -22\rightarrow22$
$k = -16\rightarrow16$
$l = -8\rightarrow8$

Refinement

Refinement on F^2
Least-squares matrix: full
$R[F^2 > 2\sigma(F^2)] = 0.038$
$wR(F^2) = 0.096$
$S = 1.11$
1670 reflections
131 parameters
4 restraints
Primary atom site location: structure-invariant direct methods
Secondary atom site location: difference Fourier map
Hydrogen site location: inferred from neighbouring sites
H atoms treated by a mixture of independent and constrained refinement

$w = 1/[\sigma^2(F_o^2) + (0.0704P)^2 + 2.8002P]$
where $P = (F_o^2 + 2F_c^2)/3$
$(\Delta/\sigma)_{max} = 0.038$
$\Delta\rho_{max} = 1.68$ e Å^{-3}
$\Delta\rho_{min} = -0.76$ e Å^{-3}

Extinction correction: SHELXL97 (Sheldrick, 2008), $Fc^* = kFc[1+0.001xFc^2\lambda^3/\sin(2\theta)]^{-1/4}$
Extinction coefficient: 0.0028 (4)
Absolute structure: Flack (1983), 731 Friedel pairs
Absolute structure parameter: −0.036 (14)

Special details

Geometry. All esds (except the esd in the dihedral angle between two l.s. planes) are estimated using the full covariance matrix. The cell esds are taken into account individually in the estimation of esds in distances, angles and torsion angles; correlations between esds in cell parameters are only used when they are defined by crystal symmetry. An approximate (isotropic) treatment of cell esds is used for estimating esds involving l.s. planes.

Refinement. Refinement of F^2 against ALL reflections. The weighted R-factor wR and goodness of fit S are based on F^2, conventional R-factors R are based on F, with F set to zero for negative F^2. The threshold expression of $F^2 > 2\text{sigma}(F^2)$ is used only for calculating R-factors(gt) etc. and is not relevant to the choice of reflections for refinement. R-factors based on F^2 are statistically about twice as large as those based on F, and R- factors based on ALL data will be even larger.

Fractional atomic coordinates and isotropic or equivalent isotropic displacement parameters (Å²)

	x	*y*	*z*	U_{iso}*/U_{eq}
Bi1	0.5000	0.35812 (2)	0.08277 (6)	0.0310 (2)
Cl1	0.36329 (14)	0.3716 (2)	0.0695 (12)	0.0685 (10)
Cl2	0.5000	0.2105 (2)	−0.1139 (6)	0.0458 (7)
Cl3	0.5000	0.2501 (3)	0.3697 (5)	0.0500 (8)
Cl4	0.5000	0.5302 (3)	0.2874 (5)	0.0652 (10)
O1W	0.6246 (4)	0.3531 (5)	0.585 (3)	0.0570 (18)
C1	0.6621 (5)	0.0963 (7)	0.7492 (14)	0.042 (2)
C2	0.6058 (5)	0.0522 (8)	0.6684 (15)	0.049 (2)
H2C	0.5704	0.0873	0.6175	0.058*
C3	0.6071 (6)	−0.0470 (8)	0.6707 (16)	0.054 (3)
H3	0.5705	−0.0804	0.6215	0.065*
C4	0.6607 (6)	−0.1001 (8)	0.7433 (16)	0.056 (2)
H4	0.6590	−0.1673	0.7390	0.067*
C5	0.7154 (7)	−0.0568 (8)	0.8201 (15)	0.047 (3)
H5	0.7511	−0.0926	0.8684	0.057*
C6	0.7153 (6)	0.0439 (9)	0.8229 (14)	0.040 (2)
N3	0.7585 (5)	0.1125 (8)	0.8909 (15)	0.050 (2)
H3A	0.7954	0.0992	0.9469	0.060*
N1	0.6790 (5)	0.1908 (7)	0.7770 (15)	0.058 (2)
H1	0.6545	0.2390	0.7434	0.070*
N2	0.7371 (5)	0.1995 (8)	0.8609 (16)	0.061 (3)
H11	0.600 (5)	0.400 (8)	0.638 (18)	0.091*
H22	0.595 (5)	0.320 (10)	0.520 (18)	0.091*

Atomic displacement parameters (Å²)

	U^{11}	U^{22}	U^{33}	U^{12}	U^{13}	U^{23}
Bi1	0.0321 (3)	0.0286 (3)	0.0323 (3)	0.000	0.000	−0.0007 (2)
Cl1	0.0362 (11)	0.0924 (19)	0.077 (3)	0.0003 (11)	0.008 (2)	−0.013 (2)
Cl2	0.0575 (19)	0.0308 (16)	0.0490 (17)	0.000	0.000	−0.0089 (14)

Cl3	0.0605 (19)	0.0469 (19)	0.0427 (16)	0.000	0.000	0.0107 (16)
Cl4	0.088 (3)	0.053 (2)	0.054 (2)	0.000	0.000	−0.0215 (16)
O1W	0.042 (3)	0.060 (5)	0.069 (5)	0.002 (2)	0.002 (10)	−0.010 (5)
C1	0.041 (5)	0.033 (5)	0.051 (5)	0.001 (4)	0.009 (4)	−0.002 (4)
C2	0.047 (5)	0.050 (6)	0.049 (5)	0.008 (4)	0.001 (4)	−0.002 (4)
C3	0.048 (5)	0.056 (7)	0.059 (6)	−0.008 (5)	−0.001 (5)	−0.011 (5)
C4	0.064 (6)	0.042 (6)	0.062 (6)	−0.004 (5)	0.016 (5)	−0.005 (5)
C5	0.053 (7)	0.042 (6)	0.047 (6)	0.011 (5)	0.002 (5)	0.001 (5)
C6	0.032 (5)	0.046 (5)	0.040 (5)	0.004 (4)	0.002 (4)	−0.007 (5)
N3	0.044 (5)	0.053 (6)	0.053 (6)	−0.002 (5)	0.005 (4)	−0.006 (4)
N1	0.052 (5)	0.037 (5)	0.085 (7)	−0.001 (4)	0.011 (5)	−0.005 (5)
N2	0.053 (6)	0.050 (6)	0.080 (7)	−0.016 (5)	0.010 (5)	−0.018 (5)

Geometric parameters (Å, º)

Bi1—Cl1	2.669 (3)	C2—H2C	0.9300
Bi1—Cl1^{i}	2.669 (3)	C3—C4	1.394 (17)
Bi1—Cl2	2.545 (3)	C3—H3	0.9300
Bi1—Cl3	2.674 (4)	C4—C5	1.358 (18)
Bi1—Cl4^{ii}	2.757 (4)	C4—H4	0.9300
Bi1—Cl4	2.856 (4)	C5—C6	1.392 (13)
Cl4—Bi1^{iii}	2.757 (4)	C5—H5	0.9300
O1W—H11	0.90 (2)	C6—N3	1.370 (15)
O1W—H22	0.90 (2)	N3—N2	1.293 (15)
C1—N1	1.364 (16)	N3—H3A	0.8600
C1—C6	1.387 (16)	N1—N2	1.308 (15)
C1—C2	1.402 (15)	N1—H1	0.8600
C2—C3	1.371 (16)		
Cl2—Bi1—Cl1	91.88 (13)	C3—C2—H2C	122.8
Cl2—Bi1—Cl1^{i}	91.88 (13)	C1—C2—H2C	122.8
Cl1—Bi1—Cl1^{i}	170.9 (2)	C2—C3—C4	123.0 (10)
Cl2—Bi1—Cl3	92.80 (16)	C2—C3—H3	118.5
Cl1—Bi1—Cl3	94.06 (17)	C4—C3—H3	118.5
Cl1^{i}—Bi1—Cl3	94.06 (17)	C5—C4—C3	122.1 (10)
Cl2—Bi1—Cl4^{ii}	87.32 (14)	C5—C4—H4	118.9
Cl1—Bi1—Cl4^{ii}	85.93 (17)	C3—C4—H4	118.9
Cl1^{i}—Bi1—Cl4^{ii}	85.93 (17)	C4—C5—C6	116.5 (12)
Cl3—Bi1—Cl4^{ii}	179.88 (13)	C4—C5—H5	121.8
Cl2—Bi1—Cl4	176.93 (13)	C6—C5—H5	121.8
Cl1—Bi1—Cl4	87.90 (13)	N3—C6—C1	104.7 (10)
Cl1^{i}—Bi1—Cl4	87.90 (13)	N3—C6—C5	134.1 (13)
Cl3—Bi1—Cl4	90.27 (13)	C1—C6—C5	121.1 (13)
Cl4^{ii}—Bi1—Cl4	89.61 (3)	N2—N3—C6	112.1 (10)
Bi1^{iii}—Cl4—Bi1	157.68 (19)	N2—N3—H3A	123.9
H11—O1W—H22	106 (3)	C6—N3—H3A	123.9
N1—C1—C6	104.8 (10)	N2—N1—C1	112.0 (10)
N1—C1—C2	132.5 (10)	N2—N1—H1	124.0

C6—C1—C2	122.7 (10)	C1—N1—H1	124.0
C3—C2—C1	114.5 (10)	N3—N2—N1	106.4 (9)

Symmetry codes: (i) −*x*+1, *y*, *z*; (ii) −*x*+1, −*y*+1, *z*−1/2; (iii) −*x*+1, −*y*+1, *z*+1/2.

Hydrogen-bond geometry (Å, º)

D—H···*A*	*D*—H	H···*A*	*D*···*A*	*D*—H···*A*
N1—H1···O1*W*	0.86	2.08	2.891 (17)	157
N3—H3*A*···O1*W*^{iv}	0.86	2.00 (2)	2.767 (18)	148
O1*W*—H11···Cl4^{iii}	0.89 (11)	2.47 (11)	3.306 (13)	157 (9)
O1*W*—H22···Cl3	0.90 (12)	2.38 (12)	3.268 (14)	169 (11)
C5—H5···Cl1^{v}	0.93	2.73	3.603 (14)	157

Symmetry codes: (iii) −*x*+1, −*y*+1, *z*+1/2; (iv) −*x*+3/2, −*y*+1/2, *z*+1/2; (v) *x*+1/2, *y*−1/2, *z*+1.